FACILE SYNTHESIS OF Ag/C MODIFIED TiO_2 NANOCOMPOSITES FOR PHOTOCATALYTIC AND ANTIBACTERIAL APPLICATIONS

Received: 21-05-2025

Le Thi Thanh Thuy[1*], Vo Thi Thanh Tuyen[2]

[1]*Faculty of Natural Sciences Education, Sai Gon University, 273 An Duong Vuong, Ward 2, District 5, Ho Chi Minh City 700000, Vietnam*

[2]*Faculty of Natural Sciences, Quy Nhon University, 170 An Duong Vuong, Quy Nhon, Binh Dinh, 55000, Vietnam*

**Email: lttthuy@sgu.edu.vn*

TÓM TẮT

TỔNG HỢP ĐƠN GIẢN VẬT LIỆU NANOCOMPOSITE TiO_2 BIẾN TÍNH Ag/C ỨNG DỤNG LÀM XÚC TÁC QUANG VÀ KHÁNG KHUẨN

Trong nghiên cứu này, vật liệu nanocomposite TiO_2 được đồng pha tạp bạc và carbon ($Ag/C@TiO_2$) đã được tổng hợp thành công bằng phương pháp sol-gel đơn giản. Các phân tích đặc trưng về cấu trúc và hình thái học thông qua các kỹ thuật XRD, SEM, TEM, EDX, FTIR, UV-Vis DRS và phân tích diện tích bề mặt BET đã xác nhận sự hình thành của cấu trúc nano mao quản với độ kết tinh cao, sự phân bố nguyên tố đồng đều và khả năng hấp thụ ánh sáng khả kiến được cải thiện. Vật liệu $Ag/C@TiO_2$ thể hiện hoạt tính quang xúc tác trong việc phân hủy methylene blue (20 mg/L) dưới chiếu xạ ánh sáng khả kiến, nhờ vào hiệu ứng hiệp đồng giữa pha tạp carbon và bạc, giúp giảm năng lượng vùng cấm và hạn chế sự tái tổ hợp cặp điện tử–lỗ trống. Các thí nghiệm bắt gốc tự do cho thấy các gốc hydroxyl, anion superoxide và lỗ trống quang sinh là những tác nhân chính tham gia vào cơ chế quang xúc tác. Ngoài ra, các đánh giá kháng khuẩn cho thấy vật liệu $Ag/C@TiO_2$ thể hiện hiệu quả ức chế vượt trội đối với Escherichia coli và Staphylococcus aureus, đặc biệt dưới chiếu sáng bằng ánh sáng khả kiến. Những kết quả này cho thấy tiềm năng của vật liệu $Ag/C@TiO_2$ như một hệ vật liệu đa chức năng hiệu quả trong xử lý môi trường và ứng dụng kháng khuẩn.

Từ khóa: *Vật liệu nanocomposite TiO_2, quang xúc tác, hoạt tính kháng khuẩn, ánh sáng khả kiến*

1. INTRODUCTION

The persistent contamination of water resources with organic pollutants and pathogenic microorganisms has become an alarming environmental and public health concern. Industrial effluents, agricultural runoff, and domestic wastewater often contained dyes, pharmaceuticals, and microbial contaminants that were difficult to degrade using conventional treatment methods [1,2]. These pollutants not only posed toxicological risks to aquatic life but also presented challenges in ensuring safe drinking water. Traditional methods such as chlorination, ozonation, and membrane filtration were either inefficient, costly, or generate harmful by-products [3]. Therefore, there was a pressing need to develop multifunctional materials capable of simultaneously degrading organic compounds and inactivating microbial agents under environmentally friendly and energy-efficient conditions.

Semiconductor-based photocatalysis emerged as a sustainable and promising solution for water purification due to its ability to harness light energy to drive redox reactions that degrade pollutants and generate reactive oxygen species (ROS) for antibacterial action [4-7]. Titanium dioxide (TiO_2) was one of the most studied photocatalysts due to its chemical stability, low toxicity, abundance, and

strong oxidative ability under UV light [8]. Nonetheless, its wide bandgap (~3.2 eV for anatase) restricted its activation to UV light, which accounts for less than 5% of the solar spectrum. Furthermore, the high rate of electron-hole recombination within TiO_2 limited its photocatalytic efficiency [9,10]. To overcome these inherent drawbacks, researchers explored doping and surface modification strategies. Among them, the incorporation of silver (Ag) nanoparticles into TiO_2 showed significant potential. Ag exhibited localized surface plasmon resonance (SPR), which allowed the material to absorb visible light and facilitates charge separation by trapping electrons, thereby enhancing photocatalytic activity under solar irradiation [11-14]. Moreover, Ag possessed well-documented broad-spectrum antibacterial properties. It disrupted bacterial membranes, inactivated essential enzymes, and interferes with DNA replication, making Ag-modified TiO_2 a dual-functional material for disinfection and pollutant degradation [15,16]. Furthermore, the integration of carbonaceous materials as supports or dopants such as activated carbon, carbon nanotubes (CNTs), and reduced graphene oxide (rGO), wasd proven to enhance the photocatalytic performance of TiO_2-based nanocomposites. Carbon materials provided high surface area, improved adsorptive interactions with organic molecules, and offerred conductive pathways for rapid electron transport, thereby reducing charge recombination [17]. Their intrinsic conductivity and stability also contributed to improved reusability and durability of the catalyst.

Therefore, this study aimed to synthesize and characterize a novel Ag/C-TiO_2 nanocomposite with enhanced photocatalytic and antibacterial activities. The primary objective was to enhance the visible-light-driven photocatalytic degradation of organic pollutants and simultaneously impart strong antibacterial activity.

2. MATERIALS AND METHODS

2.1. Materials

Titanium(IV) isopropoxide (TTIP, 97%), silver nitrate ($AgNO_3$, ≥ 99%), ethanol (EtOH, 99.5%), nitric acid (HNO_3), and deionized water (DI) were purchased from Sigma-Aldrich (USA) and used without further purification. Methylene blue (MB) and nutrient agar for antibacterial assays were also obtained from Sigma-Aldrich. Bacterial strains Escherichia coli (Gram-negative) and Staphylococcus aureus (Gram-positive) were sourced from the Laboratory of Biomass and Biofuels Research/, Ho Chi Minh University of Technology, Vietnam National University, Ho Chi Minh, Vietnam.

2.2. Synthesis of Ag/C-TiO_2 nanocomposite

The Ag/C-TiO_2 nanocomposite was synthesized using a sol-gel method followed by hydrothermal method. Initially, 34 mL of absolute ethanol was placed in a separatory funnel, and 6 mL of TTIP was slowly added under gentle stirring to ensure complete dissolution. In a separate 250 mL beaker, 17 mL of absolute ethanol was mixed with 0.4 mL of concentrated HNO_3, 1.6 mL of deionized water, and 0.18 g of $AgNO_3$. The mixture was stirred using a magnetic stirrer until the silver nitrate was completely dissolved. The ethanolic TTIP solution was then added dropwise into the Ag-containing acidic solution under continuous stirring at room temperature. The combined solution was stirred for 2h until a homogeneous and transparent sol was obtained. This sol was subsequently aged at ambient conditions for 48 hours to

form a gel. The resulting gel was transferred into a 100 mL Teflon-lined stainless steel autoclave and subjected to hydrothermal treatment at 180 °C for 10h to induce crystallization and structural development. After cooling to room temperature, the precipitate was washed thoroughly with deionized water, dried at 100 °C for 24 hours, and finally ground into a fine powder to yield the Ag/C-TiO_2 nanocomposite.

In the same manner, C/TiO_2 was synthesized via a sol-gel method followed by hydrothermal treatment, in the absence of silver. Ag/TiO_2 nanocomposite was synthesized following a sol-gel approach similar to the method described previously. TiO_2 was synthesized using the same sol-gel method, in the absence of silver.

2.3. Characterization

The structural and phase composition of the synthesized materials were analyzed using X-ray diffraction (XRD, Cu Kα radiation, λ = 1.5406 Å). Morphological features and particle size were examined using scanning electron microscopy (SEM) and transmission electron microscopy (TEM). Surface functional groups were identified using Fourier-transform infrared spectroscopy (FTIR) in the range of 400-4000 cm^{-1}. Optical properties and band gap estimation were evaluated using UV-Vis diffuse reflectance spectroscopy (UV-Vis DRS). Elemental composition and distribution of Ag were confirmed by energy-dispersive X-ray spectroscopy (EDS) coupled with e-mapping.

2.4. Photocatalytic activity

The photocatalytic performance of the samples was evaluated by the degradation of methylene blue (MB) under visible light. In each experiment, 150 mg of photocatalyst was dispersed in 100 mL of MB solution (20 mg/L) and stirred in the dark for 30 minutes to establish adsorption–desorption equilibrium. The suspension was then irradiated using a 18 W compact fluorescent lamp (λ > 420 nm) as the visible light source. At regular time intervals (every 30 minutes), 5 mL of the solution was withdrawn, centrifuged to remove the catalyst, and analyzed using a UV-Vis spectrophotometer at 664 nm. The photodegradation efficiency was calculated using Eq. (1):

$$\text{Photodegradation (\%)} = \frac{C_0 - C}{C_0} . 100 \quad (1)$$

where C_0 and C are the initial MB concentration (mg/L) at any time (min), respectively.

2.5. Antibacterial activity

The antibacterial activity was assessed using the disk diffusion method. Bacterial strains of Escherichia coli (Gram-negative) and Staphylococcus aureus (Gram-positive) were cultured on nutrient agar plates. Sterile paper disks (6 mm diameter) were impregnated with 10 mg of the test material suspended in deionized water and placed on the agar surface. The plates were incubated at 37 °C for 24 hours. The antibacterial effect was determined by measuring the diameter of the inhibition zones. All tests were conducted in triplicate.

3. RESULTS AND DISCUSSION

3.1. Characterization

3.1.1. Characterization of TiO_2, C-TiO_2, Ag-TiO_2, Ag/C@TiO_2

The X ray diffraction patterns of the synthesized materials including TiO_2, C@TiO_2, Ag/TiO_2, and Ag/C@TiO_2 were presented in **Figure 1** and demonstrated significant differences in their phase compositions. For the pure TiO_2 sample, distinct diffraction peaks appeared at 2θ = 25.29°, 37.78°, 48.00°, 53.90°,

corresponding to the (101), (004), (200) and (105) crystal planes, indicating a well-defined anatase structure [18,19]. When carbon was incorporated to form C@TiO_2, these peaks remained but showed reduced intensity and a broader background, suggesting either smaller crystallite size or an increased level of structural disorder. The presence of silver in the Ag/TiO_2 sample was confirmed by new peaks at around 2θ values of 38° and 44°, corresponding to the (111) and (200) planes of metallic silver [20]. However, upon observing the XRD pattern of Ag-doped TiO_2, it could be seen that the 2θ angle of Ag was close to the 2θ angles of TiO_2 at (004) and (200) planes. As a result, there was overlap and interference between these peaks, leading to broader and more intense peaks at these positions compared to the undoped TiO_2 sample. This indicated the successful doping of Ag into the TiO_2 structure [21-23]. These structural modifications implied that the integration of these components alters the crystallinity and might enhance the optical and antibacterial performance of the composite.

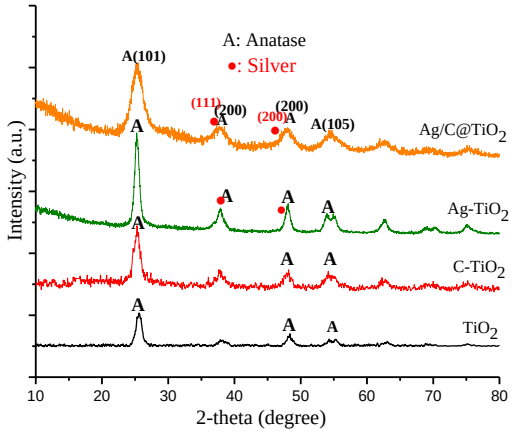

Figure 1. XRD patterns of TiO_2, C-TiO_2, Ag-TiO_2, Ag/C@TiO_2 samples

The surface morphology of TiO_2 and Ag/C@TiO_2 materials was investigated using scanning electron microscopy (SEM), as shown in **Figure 2a** and **Figure 2b**. The SEM images revealed that the synthesized catalyst particles exhibited a nanometer scale size and possessed a uniform crystalline surface. The Ag and carbon containing sample appeared darker in tone, suggesting the presence of a thin and smooth carbon coating layer. Further structural insights were obtained from transmission electron microscopy (TEM) analysis (**Figure 2c** and **Figure 2d**), which confirmed the nanostructured nature of the catalyst with particle sizes below 10 nanometers. The presence of silver was indicated by dark contrasts dispersed on the bright white TiO_2 particles. These SEM and TEM results supported the findings from X ray diffraction analysis and further confirmed the successful formation of the Ag and carbon modified TiO_2 composite.

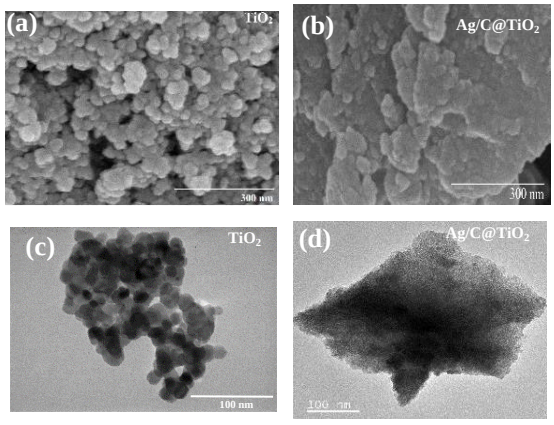

Figure 2. SEM images of TiO_2 (a);Ag/C@TiO_2 (b), and TEM images of TiO_2 (c); Ag/C@TiO_2 (d)

EDX analysis was conducted to determine the elemental composition of the synthesized samples (**Figure 3**). The results confirmed the presence of the target elements, indicating that the materials were successfully synthesized with high purity. All intended dopant elements were clearly detected in the samples, and no signals corresponding to undesired impurities were observed, further supporting the effectiveness of the synthesis method.

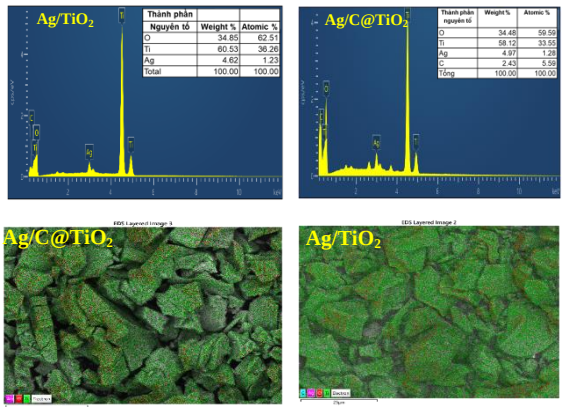

Figure 3. EDX spectra and elemental mapping of Ag/TiO_2 and $Ag/C@TiO_2$ samples

The FTIR spectra of the $Ag/C@TiO_2$ material (**Figure 4a**) confirmed the presence of characteristic functional groups. The absorption peaks at approximately 500 cm^{-1} and 1623 cm^{-1} were attributed to the bending vibrations of Ti-O and Ti-OH bonds, respectively, within the TiO_2 structure. A broad absorption band observed in the range of 3500 to 3000 cm^{-1} corresponded to the stretching vibration of hydroxyl groups from adsorbed water molecules on the material surface. Additionally, the peak at 1594 cm^{-1} indicated the presence of Ag-Ti bond vibrations, while a weak peak near 720 cm^{-1} might be associated with Ti-C bonding [24,25]. These characteristic peaks confirmed the successful incorporation of silver and carbon into the TiO_2 framework, validating the formation of the $Ag/C@TiO_2$ composite catalyst.

The optical absorption properties of TiO_2, C- TiO_2, Ag-TiO_2, and $Ag/C@TiO_2$ were evaluated using UV-Vis DRS, as shown in **Figure 4e**. The results indicated that pure TiO_2 exhibited a sharp absorption edge in the ultraviolet region. In contrast, the doped samples, particularly $Ag/C@TiO_2$, displayed an extended absorption edge toward the visible region, suggesting enhanced visible light absorption.

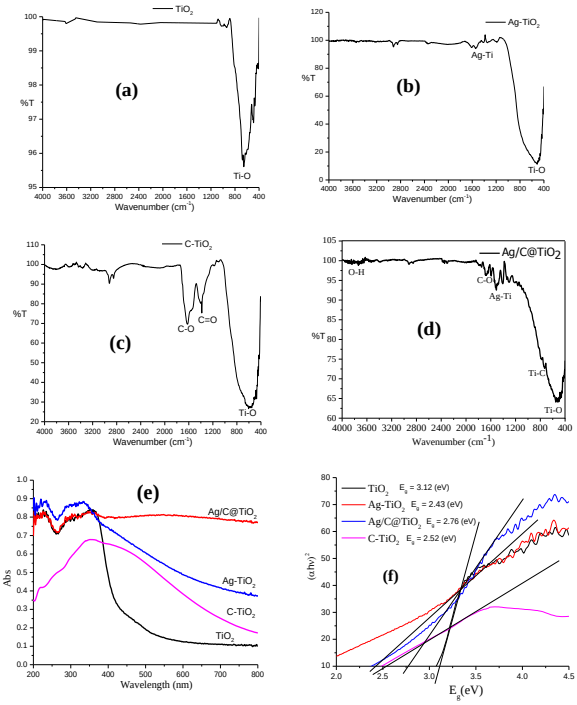

Figure 4. FTIR spectra (a-d), UV-Vis DRS spectra (e), Tauc plot (f) for the $Ag/C@TiO_2$ catalyst.

In **Figure 4f**, the optical energy gap (E_g) of the nanocomposite was determined using Tauc's plots. The results revealed the following energy band gaps (E_g) for the materials: 3.12 eV for TiO_2, 2.43 eV for TiO_2-Ag, 2.52 eV for C-TiO_2 and 2.76 eV for the $Ag/C@TiO_2$ composite. The pure TiO_2 exhibited a band gap of 3.12 eV, which was consistent with the typical values reported for anatase-phase TiO_2 [19]. Upon doping with silver nanoparticles (TiO_2-Ag), the band gap significantly decreased to 2.43 eV, indicating that Ag incorporation introduced localized energy states below the conduction band of TiO_2, thereby enhancing visible light absorption through a plasmonic effect and/or electronic coupling at the metal-semiconductor interface [26]. In particular, the ternary nanocomposite $Ag/C@TiO_2$ exhibited a band gap of 2.76 eV, which lied between those of the singly doped counterparts

[27]. This value implied a synergistic interaction between Ag and carbon within the TiO_2 matrix, balancing visible light absorption with structural stability.

This shift was attributed to the synergistic effects of Ag and C incorporation. Carbon doping might replace oxygen atoms in the TiO_2 lattice, leading to an upward shift of the valence band, while the presence of Ag nanoparticles on the surface introduced new electronic states and facilitates electron trapping, thereby narrowing the band gap energy. As a result, the Ag/C@TiO_2 composite exhibited significantly reduced band gap energy compared to the pristine and singly doped materials, as illustrated by the schematic charge transfer mechanism in **Figure 4g** [28].

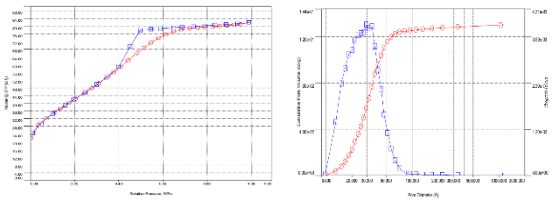

Figure 5. N_2 adsorption and desorption isotherms of the Ag/C@TiO_2 composite.

Based on the nitrogen adsorption desorption isotherms shown in **Figure 5**, all synthesized materials exhibited type IV isotherms with H3 type hysteresis loops, according to the IUPAC classification system [29, 30]. This indicateed that the Ag/C@TiO_2 composite possesses a mesoporous structure. The material exhibited a high specific surface area of 157.079 m^2/g and an average pore diameter of approximately 2.95 nm, confirming the presence of well developed mesopores. The BET analysis results demonstrated that the Ag/C@TiO_2 material had excellent adsorption capacity, making it capable of retaining active organic molecules on its surface. This enhanced the availability of catalytic active sites and facilitated the degradation of organic pollutants. Therefore, the incorporation of silver and carbon into the TiO_2 matrix not only reduced the band gap energy and suppressed the recombination of photoinduced electron hole pairs, but also improved the photocatalytic efficiency under visible light irradiation. The enhanced surface properties and mesoporous nature of the composite contributed significantly to its improved performance in environmental remediation applications.

3.2. Photocatalytic activity

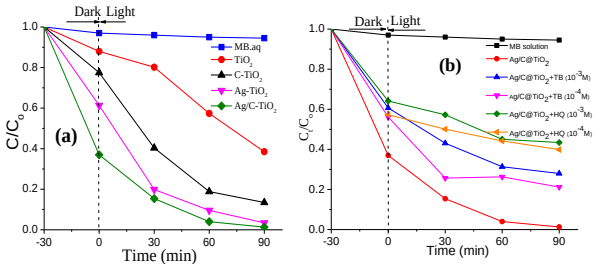

Figure 6. (a) Photocatalytic degradation of methylene blue using the TiO_2, C-TiO_2, Ag-TiO_2, Ag/C@TiO_2; (b) Photocatalytic degradation of MB in the presence of various scavengers at different molar concentrations on Ag/C@TiO_2 catalysts

The photocatalytic performance of the synthesized catalysts was evaluated by monitoring the degradation of methylene blue (MB) under visible light irradiation, as shown in **Figure 6a**. Among the samples tested, the Ag/C@TiO_2 composite exhibited the highest degradation efficiency, significantly outperforming pristine TiO_2, C-TiO_2, and Ag-TiO_2. This enhanced performance could be attributed to the synergistic effect of silver and carbon incorporation. The introduction of silver facilitates electron trapping, thereby reducing the recombination rate of photogenerated electron hole pairs. Meanwhile, carbon provided conductive pathways and enhanced visible light absorption by modifying the band

structure of TiO_2. The improved charge separation and extended light absorption spectrum collectively enhanced the photocatalytic degradation efficiency of the Ag/C@TiO_2 catalyst. The presence of Ag nanoparticles likely acted as electron sinks, facilitating interfacial charge transfer, while the carbon layer improved surface area and pollutant adsorption, further promoting photocatalytic reactions.

To better understand the photocatalytic degradation mechanism, radical scavenging experiments were conducted using the Ag/C@TiO_2 sample with different scavengers (**Figure 6b**). The degradation efficiency noticeably decreased upon the addition of scavengers, indicating the roles of specific reactive species in the photocatalytic process. In **Figure 7**, The presence of isopropanol (a hydroxyl radical scavenger) and benzoquinone (a superoxide radical scavenger) significantly inhibited MB degradation, suggesting that hydroxyl radicals (•OH) and superoxide anions ($\bullet O_2^-$) were the primary reactive species involved. Additionally, the use of ammonium oxalate (a hole scavenger) also led to a marked decrease in activity, indicating the contribution of photogenerated holes (h^+) in the degradation pathway.

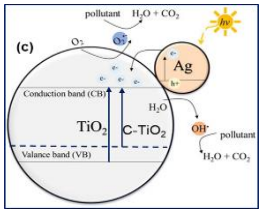

Figure 7. proposed charge transfer mechanism (g) for the Ag/C@TiO_2 catalyst.

3.3. Antibacterial activity

The antibacterial performance of the composite against Escherichia coli and Staphylococcus aureus was illustrated in **Figure 8**, with the corresponding inhibition zone diameters summarized in **Table 1**. The results showed that different composites exhibited varying degrees of antibacterial activity. Among them, the Ag/C@TiO_2 demonstrated the highest antibacterial efficacy, with inhibition zones of 11.25 ± 1.77 mm and 12.00 ± 1.41 mm against *E. coli* and *S. aureus*, respectively. In contrast, the TiO_2 and $AgNO_3$ exhibited significantly smaller inhibition zones, indicating lower antibacterial performance.

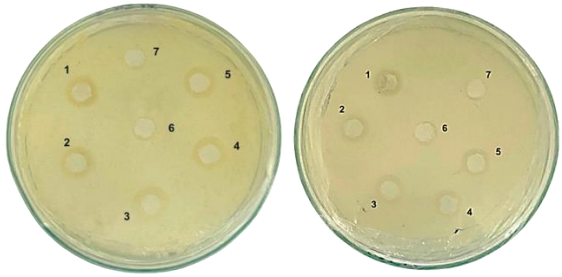

Figure 8. Inhibition zones of different samples against Escherichia coli (a) and Staphylococcus aureus (b). Sample designations: (1) Ag/C@TiO_2; (2) Ag-TiO_2; (3) C-TiO_2; (4) TiO_2; (5) $AgNO_3$; (6) Positive control; (7) Negative control.

Under visible light irradiation, the antibacterial activity of Ag/C@TiO_2, Ag-TiO_2, and C-TiO_2 was markedly enhanced. This enhancement could be attributed to the photocatalytic nature of TiO_2, a semiconductor material with a wide band gap that typically requires ultraviolet light for activation. However, doping TiO_2 with carbon and silver reducesd the band gap, effectively shifting the photocatalytic activation range into the visible spectrum. Additionally, silver nanoparticles served as effective electron mediators, facilitating charge transfer and extending the lifetime of photogenerated electron hole pairs. These long-lived charge carriers promoted the formation of highly reactive oxygen species such as hydroxyl radicals ($^{\bullet}OH$) and superoxide anions ($^{\bullet}O_2^-$), which were known to exert strong oxidative stress on microbial cells. These radicals disrupted

bacterial membranes, damage DNA, and interfered with vital cellular components, ultimately leading to bacterial cell death.

4. CONCLUSION

A multifunctional Ag and carbon modified TiO_2 nanocomposite was synthesized through a facile sol gel approach. The integration of Ag and C significantly enhanced the photocatalytic and antibacterial properties of TiO_2 by improving visible light absorption, facilitating charge separation, and extending the lifetime of reactive species. Photocatalytic experiments demonstrated that the Ag/C@TiO_2 composite achieved superior degradation efficiency for 20 mg/L of methylene blue. The incorporation of Ag and C also improved antibacterial activity effectively inhibiting the growth of E. coli and S. aureus under visible light exposure. These enhancements were attributed to the generation of reactive oxygen species and the synergistic role of Ag as a charge transfer mediator and C as a light absorber and surface stabilizer. In conclusion, the synthesized Ag/C@TiO_2 material presented a promising and cost-effective platform for future applications in wastewater treatment and antimicrobial activity.

Conflict of Interest: The authors declare that they have no conflict of interest.

Acknowledgement

This work is a part of the research project CS.2025.B2.033 funded by Saigon University.

Data availability

Data will be made available on request

References

[1] Mishra, R. K., Mentha, S. S., Misra, Y., & Dwivedi, N. (2023). Emerging pollutants of severe environmental concern in water and wastewater: A comprehensive review on current developments and future research. Water-Energy Nexus, 6, 74-95.

[2] Hübner, U., Spahr, S., Lutze, H., Wieland, A., Rüting, S., Gernjak, W., & Wenk, J. (2024). Advanced oxidation processes for water and wastewater treatment–Guidance for systematic future research. Heliyon.

[3] Saravanan, A., Deivayanai, V. C., Kumar, P. S., Rangasamy, G., Hemavathy, R. V., Harshana, T., & Alagumalai, K. (2022). A detailed review on advanced oxidation process in treatment of wastewater: Mechanism, challenges and future outlook. Chemosphere, 308, 136524.

[4] Ayodhya, D., & Veerabhadram, G. (2018). A review on recent advances in photodegradation of dyes using doped and heterojunction based semiconductor metal sulfide nanostructures for environmental protection. Materials today energy, 9, 83-113.

[5] Ayodhya, D., & Veerabhadram, G. (2018). A review on recent advances in photodegradation of dyes using doped and heterojunction based semiconductor metal sulfide nanostructures for environmental protection. Materials today energy, 9, 83-113.

[6] Chowdhury, A. P., Anantharaju, K. S., Keshavamurthy, K., & Rokhum, S. L. (2023). Recent advances in efficient photocatalytic degradation approaches for azo dyes. Journal of Chemistry, 2023(1), 9780955.

[7] Khan, S., Noor, T., Iqbal, N., & Yaqoob, L. (2024). Photocatalytic dye degradation from textile wastewater: a review. ACS omega, 9(20), 21751-21767.

[8] Fujishima, A., & Honda, K. (1972). Electrochemical photolysis of water at a semiconductor electrode. nature, 238(5358), 37-38.

[9] Zhang, J., Xu, Q., Feng, Z., Li, M., & Li, C. (2008). Importance of the relationship between surface phases and photocatalytic

activity of TiO_2. Angewandte Chemie-International Edition, 47(9), 1766-1769.

[10] Chakravorty, A., & Roy, S. (2024). A Review of-Photocatalysis, basic principles, processes, and materials. Sustainable Chemistry for the Environment, 100155.

[11] Yao, Y. C., Dai, X. R., Hu, X. Y., Huang, S. Z., & Jin, Z. (2016). Synthesis of Ag-decorated porous TiO_2 nanowires through a sunlight induced reduction method and its enhanced photocatalytic activity. Applied Surface Science, 387, 469-476.

[12] Stucchi, M., Bianchi, C. L., Argirusis, C., Pifferi, V., Neppolian, B., Cerrato, G., & Boffito, D. C. (2018). Ultrasound assisted synthesis of Ag-decorated TiO_2 active in visible light. Ultrasonics sonochemistry, 40, 282-288.

[13] Hajjaji, A., Elabidi, M., Trabelsi, K., Assadi, A. A., Bessais, B., & Rtimi, S. (2018). Bacterial adhesion and inactivation on Ag decorated TiO_2-nanotubes under visible light: Effect of the nanotubes geometry on the photocatalytic activity. Colloids and Surfaces B: Biointerfaces, 170, 92-98.

[14] Abbas, N. H., Rasuli, R., & Nakhostin Panahi, P. (2025). Decorated titanium oxide with Ag nanoparticles as an efficient photocatalyst under visible light: a novel synthesis approach. Scientific Reports, 15(1), 8207.

[15] Rai, M., Yadav, A., & Gade, A. (2009). Silver nanoparticles as a new generation of antimicrobials. Biotechnology advances, 27(1), 76-83.

[16] Harikishore, M., Sandhyarani, M., Venkateswarlu, K., Nellaippan, T. A., & Rameshbabu, N. (2014). Effect of Ag doping on antibacterial and photocatalytic activity of nanocrystalline TiO_2. Procedia materials science, 6, 557-566.

[17] Zhang, N., Zhang, Y., & Xu, Y. J. (2012). Recent progress on graphene-based photocatalysts: current status and future perspectives. Nanoscale, 4(19), 5792-5813.

[18] H. Mao, Z. Fei, C. Bian, L. Yu, S. Chen, Y. Qian, (2019). Facile synthesis of highperformance photocatalysts based on Ag/TiO_2 composites. *Ceram. Int.*, **45**, 12586–12589.

[19] Abish, V. J., Roy, A. C. H., Davidson, D. J., Raja, D. H., & Sakthivel, P. (2024). TiO_2 nanotubes as enhanced electrocatalytic oxygen evolution reaction catalyst for water splitting in alkaline medium. *Results in Surfaces and Interfaces*, **17**, 100312.

[20] Y. Zhang, F. Fu, Y. Li, D. Zhang, Y. Chen, (2018). One-step synthesis of $Ag@TiO_2$ nanoparticles for enhanced photocatalytic performance. *Nanomaterials.*, **8**, 1–15.

[21] Liu, G., Lu, Z., Zhu, X., Du, X., Hu, J., Chang, S., & Liu, Y. (2019). Facile in-situ growth of Ag/TiO2 nanoparticles on polydopamine modified bamboo with excellent mildew-proofing. *Scientific Reports*, **9(1)**, 16496.

[22] Zhang, X., Sun, H., Tan, S., Gao, J., Fu, Y., & Liu, Z. (2019). Hydrothermal synthesis of Ag nanoparticles on the nanocellulose and their antibacterial study. *Inorganic Chemistry Communications*, **100**, 44-50.

[23] Zhang, L., Lu, H., Chu, J., Ma, J., Fan, Y., Wang, Z., & Ni, Y. (2020). Lignin-directed control of silver nanoparticles with tunable size in porous lignocellulose hydrogels and their application in catalytic reduction. *ACS Sustainable Chemistry & Engineering*, **8(33)**, 12655-12663.

[24] Sahadewo, A. H., Elysabeth, T., & Slamet. (2023). Utilization of Uncaria gambir Roxb leaf extract as a reducing agent in the green synthesis of Ag/TiO_2 composites and its application for multifunctional towels. *Textile Research Journal*, **93(11-12)**, 2849-2858.

[25] Akhtar, T., Hill, A. J., Bhat, A., Schwank, J. W., Nasir, H., Bukhari, S. A. B., & Sitara, E. (2023). Fabrication of ruthenium doped $Ag@TiO_2$ core-shell

nanophotocatalyst for the efficient reduction of nitrophenols. *Applied Surface Science*, **630**, 157491.

[26] Scarisoreanu, M., Ilie, A. G., Goncearenco, E., Banici, A. M., Morjan, I. P., Dutu, E., & Fleaca, C. (2020). Ag, Au and Pt decorated TiO2 biocompatible nanospheres for UV & vis photocatalytic water treatment. *Applied Surface Science*, **509**, 145217.

[27] Lopes, F. C. S., Maria da Graça, C., Bargiela, P., Ferreira, H. S., & Pires, C. A. D. M. (2020). Ag/TiO2 photocatalyst immobilized onto modified natural fibers for photodegradation of anthracene. *Chemical Engineering Science*, **227**, 115939.

[28] Dianping Jiang , Meditha Hudandini, Yuya Masaki,K. Kusdianto, Masaru Kubo & Manabu Shimada, (2024). Visible-Light-Driven Photocatalytic Activity of Ag-Loaded TiO_2 Nanoparticulate Thin Film Fabricated via PECVD-PVD Method. *Journal of Chemical Engineering of Japan.*, 2331105.

[29] K.E. Ahmed, D.-H. Kuo, M.A. Zeleke, O.A. Zelekew, A.K. Abay, (2019). Synthesis of $SnWO_3$/g-C_3N_4 composites with surface activated oxygen for visible light degradation of dyes, *J. Photochem. Photobiol. A Chem*., **369**, 133–141.

[30] F. Guo, X. Huang, Z. Chen, H. Ren, M. Li, L., (2020). Chen, MoS_2 nanosheets anchored on porous $ZnSnO_3$ cubes as an efficient visible-light-driven composite photocatalyst for the degradation of tetracycline and mechanism insight. *J. Hazard. Mater*., **390**, 122158.

Table 1. Antibacterial activity of the samples evaluated by the agar well diffusion method. Data were presented as mean ± standard deviation, with n = 3.

No.	Sample	Inhibition zone (mm)	
		Escherichia coli	*Staphylococcus aureus*
1	Ag/C@TiO_2	11.25 ± 1.77	12.00 ± 1.41
2	Ag/TiO_2	10.50 ± 3.18	11.50 ± 0.71
3	C@TiO_2	10.75 ± 2.12	11.00 ± 1.21
4	TiO_2	10.50 ± 1.54	11.00
5	$AgNO_3$	11.00 ± 1.41	10.50 ± 0.71
6	Positive control	9.25 ± 0.35	9.25 ± 1.77
7	Negatice control	9.00	9.00